Articles

Evolution of Enzymatic Activity in the Tautomerase Superfamily: Mechanistic and Structural Consequences of the L8R Mutation in 4-Oxalocrotonate Tautomerase[†,‡]

Gerrit J. Poelarends,[§,||,⊥] Jeffrey J. Almrud,[§,||] Hector Serrano,[§] Joseph E. Darty,[#] William H. Johnson, Jr.,[§] Marvin L. Hackert,[#] and Christian P. Whitman*[,§]

Division of Medicinal Chemistry, College of Pharmacy, and Department of Chemistry and Biochemistry, The University of Texas, Austin, Texas 78712-1074

Received January 11, 2006; Revised Manuscript Received April 27, 2006

ABSTRACT: 4-Oxalocrotonate tautomerase (4-OT) and *trans*-3-chloroacrylic acid dehalogenase (CaaD) are members of the tautomerase superfamily, a group of structurally homologous proteins that share a $\beta-\alpha-\beta$ fold and a catalytic amino-terminal proline. 4-OT, from *Pseudomonas putida* mt-2, catalyzes the conversion of 2-oxo-4-hexenedioate to 2-oxo-3-hexenedioate through the dienol intermediate 2-hydroxymuconate in a catabolic pathway for aromatic hydrocarbons. CaaD, from *Pseudomonas pavonaceae* 170, catalyzes the hydrolytic dehalogenation of *trans*-3-chloroacrylate in the *trans*-1,3-dichloropropene degradation pathway. Both reactions may involve an arginine-stabilized enediolate intermediate, a capability that may partially account for the low-level CaaD activity of 4-OT. Two active-site residues in 4-OT, Leu-8 and Ile-52, have now been mutated to the positionally conserved and catalytic ones in CaaD, αArg-8, and αGlu-52. The L8R and L8R/I52E mutants show improved CaaD activity (50- and 32-fold increases in k_{cat}/K_m, respectively) and diminished 4-OT activity (5- and 1700-fold decreases in k_{cat}/K_m, respectively). The increased efficiency of L8R-4-OT for the CaaD reaction stems primarily from an 8.8-fold increase in k_{cat}, whereas that of the L8R/I52E mutant is due largely to a 23-fold decrease in K_m. The presence of the additional arginine residue in the active site of L8R-4-OT does not alter the pK_a of the Pro-1 amino group from that measured for the wild type (6.5 ± 0.1 versus 6.4 ± 0.2). Moreover, the crystal structure of L8R-4-OT is comparable to that of the wild type. Hence, the enhanced CaaD activity of L8R-4-OT is likely due to the additional arginine residue that can participate in substrate binding and/or stabilization of the putative enediolate intermediate. The results also suggest that the evolution of new functions within the tautomerase superfamily could be quite facile, requiring only a few strategically placed active-site mutations.

It has been well-documented that many enzymes exhibit catalytic promiscuity, which is the ability of an enzyme to accelerate a reaction (or reactions) in addition to its biologically relevant one (for examples, see refs *1*−*7*). These generally low-level activities may serve as starting points for the creation of new enzymatic functions. Under selective pressure, duplication of the gene for the existing enzyme followed by the introduction of a small number of mutations could enhance one of the low-level activities and lead to a new enzyme (*8*−*12*). An understanding of the sequence of events that generates new enzymes from the structural framework of pre-existing enzymes would provide insight into natural evolution and could lead to the development of useful biocatalysts.

4-Oxalocrotonate tautomerase (4-OT)[1] and *trans*-3-chloroacrylic acid dehalogenase (CaaD) catalyze very different reactions in two different biological pathways (*13*, *14*). However, they both belong to the 4-OT family of the tautomerase superfamily, a group of structurally homologous proteins that share a characteristic $\beta-\alpha-\beta$ fold and a catalytic amino-terminal proline (*13*−*16*). 4-OT, a homo-

[†] This research was supported by the National Institutes of Health Grant GM-41238 (to C.P.W.) and the Robert A. Welch Foundation (F-1334 and F-1219).

[‡] The coordinates have been deposited within the Brookhaven Protein Data Bank (PDB code 2FM7).

* To whom correspondence should be addressed: Telephone: 512-471-6198. Fax: 512-232-2606. E-mail: whitman@mail.utexas.edu.

[§] Division of Medicinal Chemistry.

[||] The authors contributed equally to this work.

[⊥] Present address: Department of Biochemistry, Groningen Biomolecular Sciences and Biotechnology Institute, University of Groningen, Nijenborgh 4, 9747 AG, Groningen, The Netherlands.

[#] Department of Chemistry and Biochemistry.

[1] Abbreviations: CHMI, 5-carboxymethyl-2-hydroxymuconate isomerase; CaaD, *trans*-3-chloroacrylic acid dehalogenase; *cis*-CaaD, *cis*-3-chloroacrylic acid dehalogenase; ESI−MS, electrospray ionization mass spectrometry; F_o and F_c, observed and calculated structure factors, respectively; HPLC, high-pressure liquid chromatography; MSAD, malonate semialdehyde decarboxylase; MIF, macrophage migration inhibitory factor; NCS, noncrystallographic symmetry; NMR, nuclear magnetic resonance; 4-OT, 4-oxalocrotonate tautomerase; PPT, phenylpyruvate tautomerase; rmsd, root-mean-square deviation.

10.1021/bi0600603 CCC: $33.50
Published on Web 06/06/2006

Scheme 1

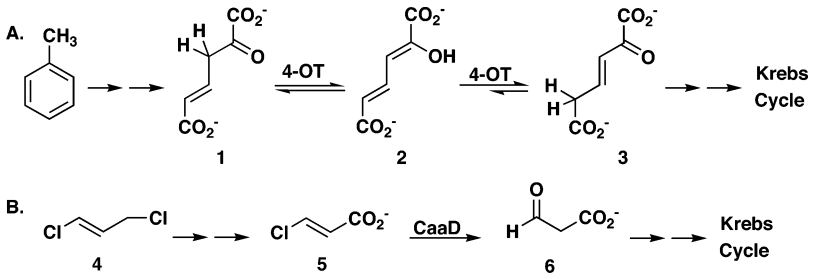

Scheme 2

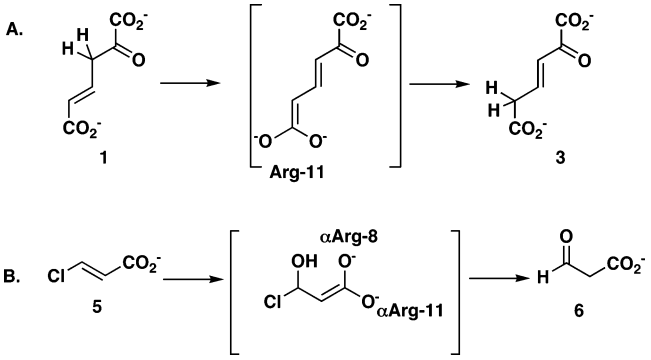

hexamer, is part of a degradation pathway for aromatic hydrocarbons such as benzene, toluene, and xylenes in the soil bacterium *Pseudomonas putida* mt-2 (*17*, *18*). The enzyme converts 2-oxo-4-hexenedioate (**1**, Scheme 1A) to 2-oxo-3-hexenedioate (**3**) through the dienol intermediate, 2-hydroxymuconate (**2**) (*19*). CaaD, a heterohexamer consisting of three α subunits and three β subunits, is found in a degradation pathway for *trans*-1,3-dichloropropene (**4**, Scheme 1B) in the soil bacterium *Pseudomonas pavonaceae* 170 (*20*, *21*). It catalyzes the hydrolytic dehalogenation of *trans*-3-chloroacrylate (**5**) to yield malonate semialdehyde (**6**) (*22*).

The mechanisms for both enzymes have been extensively characterized, and the crystal structures have been solved (*13*, *14*, *23*−*25*). A review of this body of work shows similarities between the enzymes including the common β−α−β building block, the catalytic Pro-1, and the formation of an arginine-stabilized enediolate intermediate during the reaction. In 4-OT, such an intermediate would facilitate protonation at C-5 to yield **3** (Scheme 2A) (*13*, *24*). In CaaD, the formation of an enediolate intermediate could facilitate the elimination of chloride to yield an enol intermediate (Scheme 2B) (*14*, *25*). There are also differences. The pK_a values for the amino-terminal prolines are markedly different (∼6.4 in 4-OT versus 9.2 in CaaD), and they have different roles (*26*−*28*). In 4-OT, Pro-1 functions as a general base, abstracting the proton from C-3 of **1**, whereas in CaaD, Pro-1 functions as a general acid and provides a proton to C-2 of **5**, to complete the addition of water. A second difference is the presence of the water-activating residue, Glu-52 (from the α subunit) in CaaD (*25*). Finally, an additional arginine residue (αArg-8) in CaaD is likely involved in stabilizing the enediolate intermediate (Scheme 2B) (*25*).

The presence of αArg-8 and αGlu-52 in CaaD and the absence of these two residues at comparable positions in 4-OT suggested that the reported low-level CaaD activity of 4-OT (*4*) could be improved by substituting the Leu-8 and Ile-52 residues in 4-OT for those found in CaaD. Replacement of Ile-52 with a glutamate residue might have an additional benefit: Ile-52 is part of a β hairpin, and destabilization of this structural element in 4-OT has previously been shown to make the active site more accessible to water (*13*, *15*). Accordingly, as a first step in determining whether nature can exploit the promiscuous dehalogenase activity of 4-OT and provide a selective advantage by enhancing this activity, three 4-OT mutants (L8R, I52E, and L8R/I52E) were constructed and their properties were investigated. Two 4-OT mutants, L8R and L8R/I52E, show an increase in catalytic efficiency for the CaaD reaction largely because of an increase in k_{cat} (L8R-4-OT) or a decrease in K_m (L8R/I52E). Further characterization of L8R-4-OT, the mutant with the highest catalytic efficiency for the CaaD reaction, suggests that the improved activity is due to the participation of the additional arginine residue in substrate binding and/or stabilization of the putative enediolate intermediate. In addition to reinforcing the hypothesis that the tautomerase superfamily represents divergent evolution from a common ancestor, the results demonstrate the facile adaptability of the β−α−β fold in that relatively minor changes in the active site of one tautomerase superfamily member can significantly improve the catalytic efficiency of a very different reaction.

EXPERIMENTAL PROCEDURES

Materials. Chemicals, biochemicals, buffers, and solvents were purchased from Sigma−Aldrich Chemical Co. (St. Louis, MO), Fisher Scientific, Inc. (Pittsburgh, PA), Fluka Chemical Co. (Milwaukee, WI), or EM Science (Cincinnati, OH). The synthesis of 2-hydroxymuconate (**2**) is reported elsewhere (*19*). The sources for the components of Luria−Bertani (LB) media as well as the enzymes and reagents used in the molecular-biology procedures are reported elsewhere (*16*). The Amicon stirred cells and the YM3 and YM10 ultrafiltration membranes were obtained from Millipore Co. (Billerica, MA). Oligonucleotides for DNA amplification and sequencing were synthesized by Genosys (The Woodlands, TX).

General Methods. Absorbance data were obtained on a Hewlett−Packard 8452A diode array spectrophotometer. Kinetic parameters were calculated from a fit of the initial velocity data at different substrate concentrations to the Michaelis−Menten equation by using the Grafit program (Erithacus Software Ltd., Horley, U.K.) obtained from Sigma Chemical Co.

Construction, Overexpression, and Purification of the 4-OT Mutants. The experimental procedures used for the construction of the 4-OT mutants and their overexpression and purification are provided in the Supporting Information.

Mass Spectrometric Characterization of 4-OT, the 4-OT Mutants, and ^{15}N-Labeled L8R-4-OT. The masses of 4-OT, the three 4-OT mutants, and ^{15}N-labeled L8R-4-OT were determined using an LCQ electrospray ion-trap mass spectrometer (ThermoFinnigan, San Jose, CA), housed in the Analytical Instrumentation Facility Core in the College of Pharmacy at the University of Texas at Austin. The protein samples were made up as described elsewhere (*22*). The observed monomer mass for 4-OT was 6810 Da (calcd 6811 Da). The observed monomer mass for the L8R mutant was 6853 Da (calcd 6854 Da); that of the I52E mutant was 6826 Da (calcd 6827 Da); and that of the L8R/I52E mutant was 6869 Da (calcd 6870 Da). The observed monomer mass for the uniformly ^{15}N-labeled L8R-4-OT was 6945 Da (calcd 6945 Da).

Enzyme Assays. The ketonization of **2** by the 4-OT mutant enzymes was monitored by following the formation of **3** at 236 nm ($\epsilon = 6580$ M^{-1} cm^{-1}) in 20 mM NaH_2PO_4 buffer (pH 7.3) as reported (*19*). An aliquot of each enzyme was diluted into 20 mL of 20 mM NaH_2PO_4 buffer at pH 7.3, yielding a final monomer concentration of 1.8 nM (L8R), 4.3 nM (I52E), and 2.9 μM (L8R/I52E). The diluted enzyme was incubated for 60 min at 23 °C. Subsequently, 1 mL aliquots were transferred to a cuvette, and the assay was initiated by the addition of a small quantity (1−8 μL) of **2** from a 50 mM stock solution made in ethanol. The concentrations of substrate used in the assay ranged from 0 to 400 μM.

The dehalogenation of **5** was monitored by following the release of halide in 50 mM Tris-SO_4 buffer (pH 8.2) using a colorimetric assay (*21*, *29*). An aliquot of enzyme was diluted into 50 mM Tris-SO_4 buffer (pH 8.2), yielding a final monomer concentration of 27 μM (4-OT), 22 μM (L8R), 22 μM (I52E), and 15 μM (L8R/I52E). The diluted enzyme solutions were incubated for at least 60 min at 23 °C. Subsequently, a 100 μL portion of the enzyme solution was transferred to a tube containing the desired concentration of substrate in 2.9 mL of 50 mM Tris-SO_4 buffer (pH 8.2). The concentrations of substrate used in the assay ranged from 0 to 200 mM. Substrate was added from a stock solution that was made up in 50 mM Tris-SO_4 buffer. The pH of the stock solution was adjusted to 8.2. Halide concentrations were measured colorimetrically at different time intervals. The kinetic parameters presented in Table 1 correspond to two independent measurements.

^{1}H Nuclear Magnetic Resonance (NMR) Spectroscopic Detection of Malonate Semialdehyde in the L8R- and L8R/I52E-Catalyzed Transformation of ***5***. A series of ^{1}H NMR spectra monitoring the L8R- and L8R/I52E-catalyzed transformation of **5** were recorded as reported (*22*), using the following conditions. An amount of **5** (4 mg, 0.04 mmol) dissolved in DMSO-d_6 (30 μL) was added to 100 mM Na_2HPO_4 buffer (0.6 mL, pH ∼ 9) and placed in an NMR tube. The addition of **5** lowered the pH of the reaction mixture. Hence, the pH was adjusted to 8.0 using small aliquots of a 10 M NaOH solution. Subsequently, an aliquot of either L8R (100 μL of a 30 mg/mL solution made up in 20 mM Na_2HPO_4 buffer at pH 7.3) or L8R/I52E (150 μL of a 20 mg/mL solution made up in 20 mM Na_2HPO_4 buffer at pH 7.3) was added to the reaction mixture. The first ^{1}H NMR spectrum was recorded 5 min after the addition of enzyme and every 10 min thereafter for a total reaction time of 95 min. The final pH of the reaction mixture was 7.3. The signals for **5**, the hydrate of **6**, acetaldehyde, and the hydrate of acetaldehyde are reported elsewhere (*22*). The signals for the methylene protons of **6** are obscured by the large amount of protein in the sample.

NMR Titration Experiments. The L8R-4-OT was uniformly ^{15}N-labeled as described previously (*26*, *28*). The final yield of homogeneous ^{15}N-labeled L8R-4-OT per liter of culture was ∼4 mg. The pK_a of the amino group of the N-terminal proline was determined by monitoring the pH dependence of the ^{15}N chemical shift of the secondary amino nitrogen resonance. Spectra were acquired on a Varian Inova 500 MHz spectrometer using an inverse broad-band probe configured for ^{15}N 1D NMR spectroscopy without proton decoupling. The ^{15}N chemical shifts were referenced to external liquid ammonia as described (*30*). The titrations were performed at 27 °C, using a uniformly ^{15}N-labeled L8R sample, which was 3.6 mM in subunits in 10 mM sodium phosphate buffer (containing 10% D_2O), by adding small aliquots (typically 1 μL) of 1 M HCl or NaOH to the sample. The titrations were performed in the pH range of 5.06−9.11, and the enzyme retained nearly full activity at the end of the experiment. The acquisition parameters were as follows: spectral width, 10 371 Hz; acquisition time, 1.998 s; relaxation delay, 2 s; total numer of transients, 1500−2500; and flip angle, 90°. To obtain the pK_a of Pro-1, the data obtained from the NMR titration curve were fit using the appropriate equation for a single pK_a provided in the Grafit Program and using a lower pH limit of 55.90 ± 0.24 ppm and a higher pH limit of 48.26 ± 0.17 ppm.

Determination of the Crystal Structure of L8R-4-OT. Crystals of the L8R mutant were grown at 21 °C using the sitting-drop vapor diffusion method. Drops were composed of 3 μL of protein (20 mg/mL solution in 10 mM Tris-Cl at pH 7.0) mixed with an equal volume of reservoir buffer [30% *O*-(2-aminopropyl)-*O*′-(2-methoxyethyl)polypropylene glycol 500, 100 mM 2-(*N*-morpholino)ethanesulfonic acid at pH 6.5, and 50 mM CsCl]. The resulting mixture was allowed to equilibrate against 50 μL of reservoir solution. A single crystal (0.15 × 0.15 × 0.2 mm) was harvested using a Hampton Research Cryoloop, flash-cooled in liquid nitrogen, and then mounted in the nitrogen gas stream. A diffraction data set to 2.8 Å resolution was collected from this crystal at −173 °C using a Rigaku RU-H3R generator and an R-axis HTC detector. Diffraction data were integrated and scaled using HKL2000 (*31*). The crystal belongs to space group $P6_3$ with unit-cell dimensions of $a = b = 80.9$ and $c = 117.0$ Å. Assuming six monomers in the asymmetric unit, the Matthews' coefficient (*32*) is 2.7 Å^3/Da and the solvent content is 54%, respectively. The CCP4 Suite program MOLREP (*33*) was used to solve the structure of mutant L8R by molecular replacement using a wild-type 4-OT dimer, without water molecules, as the search model. In the search model, the side chain for residue 8 was truncated past C_β. The first two rounds of structure refinement were carried out using REFMAC5 and imposing strict noncrystallographic symmetry (NCS) (*34*, *35*). The resulting atomic model was then improved by iterations of maximum-likelihood refinement using CNSsolve (*36*), followed by manual intervention using the program O. The observation of positive electron density in $F_o - F_c$ maps allowed the side chain of Arg-8 to be modeled into the active site. In the final rounds of

Scheme 3

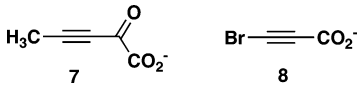

refinement, ordered water molecules were added using the water-picking routine of CNSsolve. Late-stage refinement consisted of maximum-likelihood refinement using REFMAC5 and manual intervention using the program O. The stereochemistry of the model was checked with PROCHECK (*37*). Figures were generated using MOLSCRIPT (*38*) and RASTER3D (*39*).

RESULTS

Rationale for Mutagenesis. The previously reported superpositioning of the structures of 4-OT inactivated by 2-oxo-3-pentynoate (**7**, Scheme 3) and CaaD inactivated by 3-bromopropiolate (**8**, Scheme 3) (*25*), coupled with the available mechanistic work, identified two substitutions that could enhance the low-level CaaD activity of 4-OT. The position of Leu-8 in 4-OT is structurally homologous to that of αArg-8 in CaaD, which, along with αArg-11, is postulated to bind the substrate (i.e., **5**) and stabilize an enediolate intermediate (Scheme 2B). Hence, mutation of Leu-8 to an arginine in 4-OT might improve the binding of **5** and allow for a more effective stabilization of the enediolate intermediate, assuming no structural changes accompany the mutation. The comparison also shows that the position of Ile-52 in 4-OT is structurally homologous to that of αGlu-52 in CaaD. αGlu-52 is proposed to activate a water molecule for the nucleophilic addition to C-3 of **5** (*25*). αGlu-52 is at the N-terminal part of the β hairpin, which covers the active-site pocket of CaaD and stabilizes the CaaD oligomer structure. These observations suggest that changing Ile-52 to a glutamate might provide 4-OT with a mechanism to activate a water molecule. Moreover, it has previously been shown that changing Phe-50, which precedes the β hairpin in 4-OT, to an alanine, makes the region around Pro-1 more accessible to water and increases the pK_a of the amino group of Pro-1 (*13*, *40*). Finally, it was anticipated that the double mutant (L8R/I52E) of 4-OT could improve the CaaD activity of 4-OT by a combination of the predicted effects for the single mutants.

Characterization of the 4-OT Mutants. The wild-type enzyme and the three 4-OT mutants (L8R, I52E, and L8R/I52E) were overexpressed in *Escherichia coli* strain BL21-Gold(DE3) and purified to >95% homogeneity, as assessed by sodium dodecyl sulfate−polyacrylamide gel electrophoresis (SDS−PAGE). The yields of the four enzymes varied from 30 to 50 mg (per liter of cell culture). DNA sequencing verified that only the intended mutations had been introduced into each mutant gene. Mass spectral analysis of the individual proteins showed one major peak corresponding to the expected subunit molecular mass of a 62 amino acid species. This observation confirmed that, in all cases, the initiating methionine had been removed in a post-translational process to yield a protein with an N-terminal proline. The mutant enzymes and the wild-type 4-OT migrated comparably on a gel-filtration column, which suggests that the three mutants exist as hexamers in solution.

The CaaD Activity of 4-OT and the 4-OT Mutants. The steady-state kinetic parameters for the dehalogenation of **5** by wild-type 4-OT and the three mutant enzymes are shown in Table 1. 4-OT has a low-level CaaD activity, measured by a coupled enzyme system, as previously reported (*4*). In this study, the low-level CaaD activity was determined using a more direct colorimetric assay for halide release. The low-level activities are comparable for the two assays with a minor discrepancy in the K_m values. The L8R mutant shows the highest increase in catalytic efficiency (50-fold increase in k_{cat}/K_m), which can be attributed to the 8.8-fold increase in k_{cat} along with the 5.7-fold decrease in K_m. The double mutant (L8R/I52E-4-OT) also showed improved catalytic efficiency (~32-fold increase in k_{cat}/K_m), which results primarily from the 23-fold decrease in K_m. The slight increase in k_{cat} is not likely significant. Finally, the catalytic efficiency of the I52E mutant is, at best, comparable to that of the wild type.

Table 1: Kinetic Parameters for the Dehalogenation of **5** by CaaD, 4-OT, and the 4-OT Mutants

enzyme	k_{cat} (s^{-1})	K_m (mM)	k_{cat}/K_m (s^{-1} M^{-1})
CaaD[a]	3.8 ± 0.1	$(31 \pm 2) \times 10^{-3}$	1.2×10^5
4-OT[b]	$(1.0 \pm 0.2) \times 10^{-3}$	91 ± 34	1.1×10^{-2}
L8R	$(8.8 \pm 0.3) \times 10^{-3}$	16 ± 1	5.5×10^{-1}
I52E	$(0.32 \pm 0.03) \times 10^{-3}$	59 ± 14	5.4×10^{-3}
L8R/I52E	$(1.4 \pm 0.2) \times 10^{-3}$	4 ± 2	3.5×10^{-1}

[a] These kinetic parameters were obtained from Wang et al. (*22*). [b] The steady-state kinetic parameters of 4-OT and its mutants were determined in 50 mM Tris-SO_4 buffer (pH 8.2) at 23 °C. Errors are standard deviations.

^{1}H NMR Characterization of the L8R- and L8R/I52E-4-OT-Catalyzed Reactions. Mixtures containing either the L8R or L8R/I52E mutant and **5** were monitored by ^{1}H NMR spectroscopy to verify that the product of each reaction is malonate semialdehyde (**6**), as has been previously established for the CaaD-catalyzed reaction (*22*). The ^{1}H NMR spectrum of **5** in 100 mM Na_2HPO_4 buffer (pH 8.0) shows two doublets (6.09 and 6.89 ppm), corresponding to the C-2 and C-3 protons, respectively (data not shown). After incubation of **5** with either the L8R- or L8R/I52E-4-OT for 95 min, the intensity of these signals diminishes and six new signals appear. Two signals (a doublet at 2.34 ppm and a triplet at 5.15 ppm) correspond to the hydrate of malonate semialdehyde. The other four signals are due to the presence of acetaldehyde (2.04 and 9.48 ppm) and its hydrate (1.13 and 5.05 ppm), which result from either the enzymatic or nonenzymatic decarboxylation of **6**. Hence, **6** is the product of the L8R and L8R/I52E-catalyzed conversion of **5**.

It is interesting to note that, when the incubation mixture containing wild-type 4-OT and **5** was monitored by ^{1}H NMR spectroscopy, the signals corresponding to acetaldehyde and its hydrate were observed but those corresponding to **6** and its hydrate were not (*4*). The absence of the latter signals reflects the fact that **6** is not sufficiently stable to accumulate in quantities detectable by ^{1}H NMR spectroscopy during the lengthy incubation period (136 h) required for the dehalogenation of **5** by wild-type 4-OT. In contrast, the L8R and L8R/I52E mutants of 4-OT catalyze the dehalogenation reaction at a sufficiently rapid rate that the signals for the hydrate of **6** are detected. These observations are consistent with the kinetic data and reflect an enhanced rate of dehalogenation for these two mutants.

4-OT Activity of the Mutants. The steady-state parameters for the ketonization of 2-hydroxymuconate (**2**) to 2-oxo-3-

Table 2: Kinetic Parameters for the Ketonization of **2** to **3** by 4-OT and the 4-OT Mutants[a]

enzyme	k_{cat} (s^{-1})	K_m (μM)	k_{cat}/K_m (M^{-1} s^{-1})
4-OT[b]	3500 ± 500	180 ± 30	1.9×10^7
L8R	61 ± 9	17 ± 3	3.6×10^6
I52E	32 ± 2	62 ± 13	5.2×10^5
L8R/I52E	0.3 ± 0.05	27 ± 6	1.1×10^4

[a] The steady-state kinetic parameters were determined in 20 mM sodium phosphate buffer (pH 7.3) at 23 °C. Errors are standard deviations. [b] These kinetic parameters were obtained from Harris et al. (*41*).

Table 3: Data Collection and Refinement Statistics

data collection and processing	
crystal−film distance (cm)	117
oscillation angle (deg)	0.5
exposure time (min)	5
resolution range (Å)	34.0−2.8
total measurements	496 944
unique reflections	10 782
completeness (%)	99.9
R_{sym} (%)	16.2
(I/σ)	15.7
refinement statistics	
resolution range (Å)	34.0−2.8
R_{cryst}/R_{free} (%)	23.0/30.1
rmsd bond lengths (Å)	0.022
rmsd angles (deg)	2.155
number of atoms (protein/water)	2795/199
average *B* factors (protein/water) (Å^2)	26.2/20.5

hexenedioate (**3**) by the three mutants were determined and compared to those previously determined for the wild type. All three mutants catalyze the reaction, although less efficiently than the wild type (Table 2). The most dramatic decrease in the catalytic efficiency for the wild-type activity is seen for L8R/I52E-4-OT, which shows a 1730-fold decrease in k_{cat}/K_m. There is a ~11 700-fold decrease in k_{cat} coupled with a 6.7-fold decrease in K_m. The I52E mutation causes a 36-fold decrease in k_{cat}/K_m, which results from a ~110-fold decrease in k_{cat} and a ~3-fold decrease in K_m. The L8R mutation has the least effect on the wild-type activity with a ~5.3-fold decrease in k_{cat}/K_m, resulting from a 57-fold decrease in k_{cat} and an ~11-fold decrease in K_m.

The Crystal Structure of L8R-4-OT. The structural consequences of the L8R mutation were examined by determining the X-ray crystal structure to a resolution of 2.8 Å (Table 3). The crystallographic *R* factor for the final model was 23.0% (R_{free} = 30.1%). The relatively high R_{free} value is due to the relatively low-resolution nature of the data (2.8 Å), which probably results from the large unit-cell size and the fact that there are three dimers per asymmetric unit. Nonetheless, a comparison of the L8R structure with that of the wild type (PDB accession code 4OTB) shows only local and minor effects resulting from the mutation, leaving the overall active-site architecture otherwise unchanged (Figure 1). Thus, the changes in the kinetic parameters for the 4-OT activity are not due to major structural changes. Arg-8 adopts the same conformation in all monomers, where there is well-defined electron density for this side chain (11 of 12 monomers). The overall α carbons between the wild-type enzyme and the L8R mutant protein superimpose with a root-mean-square deviation (rmsd) of 0.50 Å, and those for the residues contributing to the active site (residues 1−2, 7−11, 31−41, and 45−52) superimpose with a rmsd of 0.45 Å.

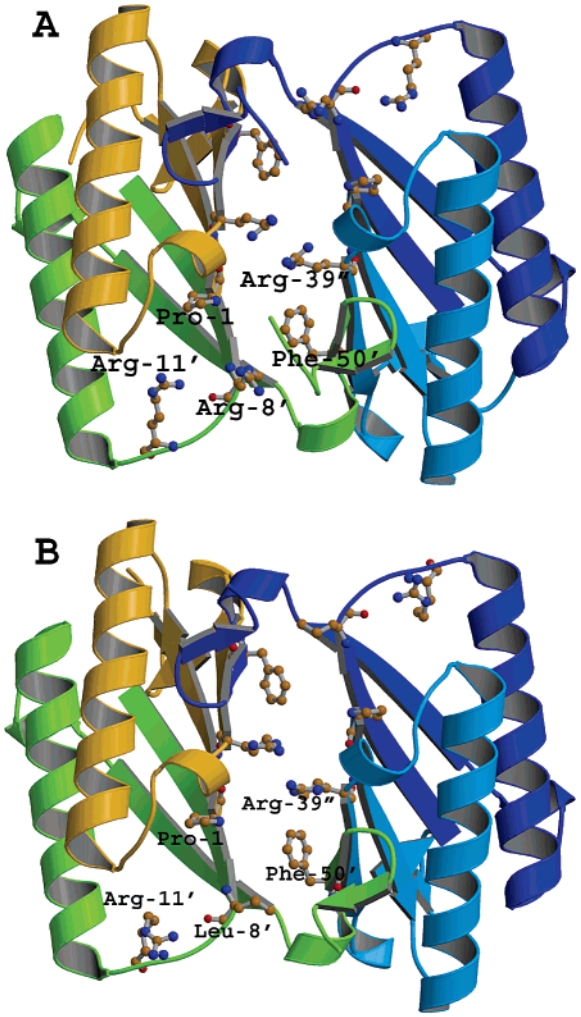

FIGURE 1: Comparison of (A) the crystal structure of the L8R-4-OT and (B) the crystal structure of wild-type 4-OT (PDB accession code 4OTB). The figure shows one active site in each structure. Except for the replacement of Leu-8 with arginine, the two structures are comparable. Ile-52 is located above Phe-50 in the 4-OT structure and near the side-chain carbon atoms of Arg-39″. The movement of Arg-11 in the L8R-4-OT structure is likely due to the fact that Arg-11 is a surface residue and is responding to a different environment.

^{15}N NMR Titration of Pro-1 in the L8R-4-OT Mutant. In 4-OT, Pro-1 functions as a base because it has a pK_a of 6.4 ± 0.2, which is due, in part, to the fact that it is surrounded by hydrophobic groups (*27*, *40*, *41*). To investigate whether the presence of the positively charged arginine residue alters the pK_a of Pro-1 in the L8R mutant, the pK_a value of this residue was measured by direct pH titration of the uniformly ^{15}N-labeled enzyme using ^{15}N NMR spectroscopy. The ^{15}N chemical shift of Pro-1 is resolved from the other ^{15}N resonances of L8R-4-OT over the pH range of 5.06−9.11, and pH titration monitoring using this resonance yields a pK_a value of 6.5 ± 0.1 (Figure 2). Thus, the additional arginine does not affect the pK_a of Pro-1.

DISCUSSION

4-OT and CaaD are members of the 4-OT family, which is one of the five known families of the tautomerase superfamily (*13*, *15*, *16*, *42*, *43*). The remaining four families are represented by their title enzymes and include *cis*-3-chloroacrylic acid dehalogenase (*cis*-CaaD) (*16*), malonate

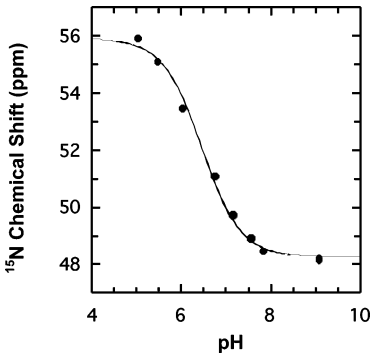

FIGURE 2: pH titration curve displaying the ^{15}N chemical shift of the amino group of Pro-1 of L8R-4-OT versus pH. The data from this plot were used to calculate the pK_a of the amino proton of Pro-1, which is reported in the text.

Scheme 4

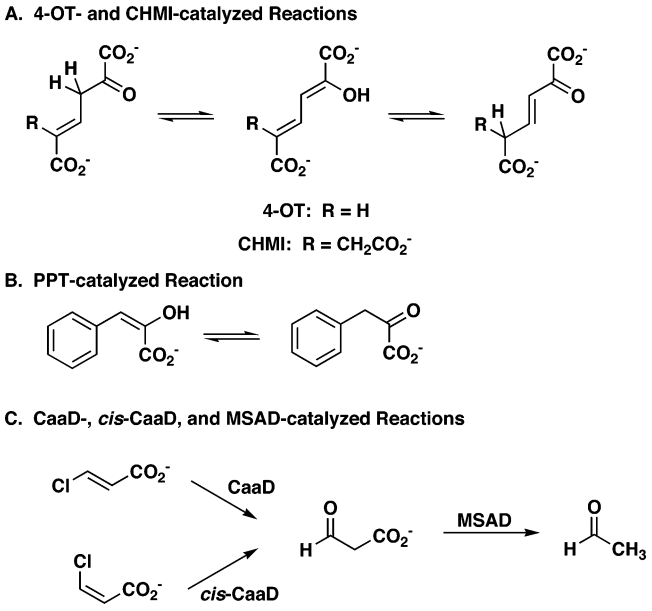

semialdehyde decarboxylase (MSAD) (*43*), 5-carboxymethyl-2-hydroxymuconate isomerase (CHMI) (*13*, *23*), and macrophage migration inhibitory factor (MIF) (*44*). *cis*-CaaD, as indicated by its name, is responsible for dehalogenation of the *cis* isomer of 3-chloroacrylate (*16*). MSAD converts **6** to acetaldehyde and follows both CaaD and *cis*-CaaD in the 1,3-dichloropropene degradation pathway (*20*). CHMI, from *E. coli C*, functions as a tautomerase in a degradation pathway for aromatic amino acids (*45*). MIF is a mammalian cytokine with a phenylpyruvate tautomerase (PPT) activity (*44*). A summary of the reactions in the tautomerase superfamily is shown in Scheme 4. All four proteins (*cis*-CaaD, MSAD, CHMI, and MIF) are homotrimers consisting of subunits that are roughly twice as long as those of 4-OT and CaaD (*16*, *23*, *25*, *46*, *47*). The monomers of these proteins have two covalently linked $\beta-\alpha-\beta$ motifs and resemble the 4-OT dimer and CaaD heterodimer.

To date, catalytic promiscuity has been identified and characterized for 4-OT, YwhB, a 4-OT family member found in *Bacillus subtilis* (*4*, *13*), CaaD (*22*), *cis*-CaaD (*16*), and MSAD (*5*). The tautomerases 4-OT and YwhB exhibit a low-level CaaD activity, which is ~10^6-fold less than that of wild-type CaaD (comparing k_{cat}/K_m values using **5**) (*4*). 4-OT also shows a low-level *cis*-CaaD activity, although kinetic

Scheme 5

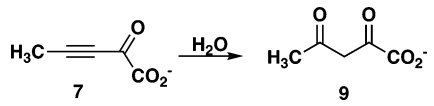

Scheme 6

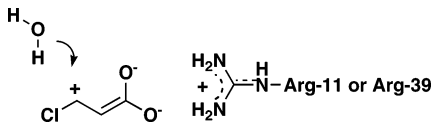

parameters have not been determined (*4*). CaaD, *cis*-CaaD, and MSAD have a promiscuous hydratase activity, converting 2-oxo-3-pentynoate (**7**, Scheme 5) to acetopyruvate (**9**) (*5*, *16*, *22*). The catalytic efficiency of these reactions varies considerably ranging from 6400 M^{-1} s^{-1} for CaaD (*22*) to 11 M^{-1} s^{-1} for *cis*-CaaD (*16*). MSAD falls in between with a k_{cat}/K_m of 600 M^{-1} s^{-1} (*5*). MSAD also catalyzes the dehalogenation of **5** at a rate that is 2×10^5-fold slower than that reported for CaaD (*5*). The observation of catalytic promiscuity in these superfamily members provides evidence for their divergent evolution from a common ancestor and highlights the evolutionary potential of the common $\beta-\alpha-\beta$ structural motif.

With regard to the CaaD activity of 4-OT, the available evidence suggests three possible mechanisms (*4*). In all three mechanisms, a positively charged residue in the active site of 4-OT (e.g., Arg-11 or Arg-39) may interact with the C-1 carboxylate group of **5** and polarize the α,β-unsaturated acid to leave a partial positive charge at C-3 (Scheme 6). Polarization facilitates the Michael addition of water to **5**. In one variation on this mechanism, Pro-1 functions as a general base and assists in the activation of a fortuitously located water molecule. Subsequently, Pro-1, now a general acid, could complete the conjugate addition of water to **5** by adding a proton at C-2. In a third mechanism, the addition of water to **5** could be completed by Pro-1 functioning as a general acid catalyst (although very little of the enzyme would exist in this form).

These mechanisms and the observed differences between CaaD and 4-OT suggested that the low-level CaaD activity of 4-OT could be improved by three modifications to the 4-OT framework. The first and most straightforward modification is to replace Leu-8 with an arginine, thereby providing additional electrostatic interactions for binding the substrate and stabilization of the enediolate intermediate. The second modification is to incorporate a mechanism for the activation of the water molecule (i.e., I52E). Finally, making the 4-OT active site more accessible to water (i.e., I52E) could facilitate a hydration reaction. The L8R mutation is the more likely one to occur in natural evolution because the codon for Leu-8 in 4-OT, CTT, requires only a single-point mutation to produce an arginine (CGT). In contrast, the codon for Ile-52, ATC, requires three point mutations to generate a glutamate (GAA or GAG).

Of the three modifications made to the 4-OT framework, the L8R mutation was the most successful one and the most easily rationalized. In view of the observations that the overall protein and active-site structures and the pK_a of Pro-1 are not changed by the incorporation of an arginine, the increase in activity (as indicated by the k_{cat} value) likely

results from a more efficient stabilization of the enediolate intermediate. The decrease in the K_m value may reflect the enhanced binding of **5** to the enzyme, assuming that the value of K_m is a measure of substrate binding. The double mutant also enhanced the CaaD activity of 4-OT but not in the expected manner: the improved catalytic efficiency is due largely to the significant decrease in K_m. It appears that the double mutant has altered the active-site cavity such that the affinity for the substrate (i.e., **5**) increases (assuming that the value of K_m reflects substrate binding). The single mutant (I52E) also decreases K_m but not as significantly as the double mutant. In the absence of a structural analysis, it is not possible to be specific about how these mutations result in an increased affinity for the substrate.

The CaaD activities of 4-OT and L8R-4-OT may appear modest at first. However, both are significantly more robust when viewed in the context of the uncatalyzed rate of hydration of **5**. Horvat and Wolfenden recently reported that the uncatalyzed reaction proceeds at a rate of 2.2×10^{-12} s^{-1} at 25 °C, indicating that CaaD provides a 10^{12}-fold rate enhancement (*48*). A comparison of the k_{cat} values for the CaaD activities of 4-OT and L8R-4-OT with this uncatalyzed rate shows that 4-OT enhances the reaction 10^8-fold and L8R-4-OT enhances the reaction 10^9-fold. Hence, a "fully active" CaaD requires only an additional 1000-fold rate enhancement.

An examination of the kinetic properties of the mutants for the wild-type activity shows that the introduction of polar residues into the active site produces significant decreases in k_{cat} and K_m. The overall effect on the catalytic efficiency is minimal for the single mutants (L8R and I52E) but is more substantial for the double mutant. The decrease in K_m for the L8R and L8R/I52E mutants could result from the presence of the additional positive charge in the active site and, along with Arg-11 and Arg-39, add to or enhance the electrostatic interactions between the enzyme and the dicarboxylate substrate. The basis for the decrease in the K_m for the I52E mutant is not immediately apparent in the absence of a structural analysis. The decrease in k_{cat} for all three mutants could be due to an effect on the reaction chemistry, product release, or both. For the L8R mutant, the decrease in k_{cat} is not due to a change in the basicity of the Pro-1 nitrogen. Instead, it may be due to an increased affinity of the enzyme for the dicarboxylate product, which would affect product release. In addition, the substrate may not be optimally aligned for proton transfer. For the I52E mutant, the negatively charged group may hinder the formation of the enolate intermediate and, along with other factors listed above, may contribute to a decrease in k_{cat}. For both the I52E and L8R/I52E mutants, a change in the pK_a of Pro-1 cannot be ruled out.

Promiscuous activities are proposed to play a key role in the evolution of new enzymes (*3*, *8*−*10*). Establishing that one or a few mutations can significantly increase the generally low-level activities may indicate that they could be used as starting points for the evolution of new functions. The enhancement of a low-level activity in an enzyme, however, can have different consequences for the original activity, with implications for how new enzymatic functions evolve (*49*, *50*). For example, Gerlt and colleagues investigated wild-type and promiscuous (evolved) activities catalyzed by two different enolase superfamily members, L-Ala-D/L-Glu epimerase (AEE) and muconate-lactonizing enzyme (MLE). Using rational design, it was found that the *o*-succinylbenzoate synthase (OSBS) activity of AEE could be generated and substantially improved by two point mutations but the original AEE activity is almost completely lost (*49*). In contrast, the promiscuous OSBS activity of MLE could be generated by a single-point mutation, selected through directed evolution, without a significant loss of the original MLE activity. It is important to note that, in the latter case, there was only selection for the generation of the promiscuous activity but no selection pressure for a decrease in the wild-type activity (*49*). An excellent overview of different enzyme mutants exhibiting large improvements in promiscuous activities and small changes in wild-type activity was recently presented by Tawfik and co-workers (*12*). The observations with AEE indicated that gene duplication is a necessary first step in the evolution of a new function so that the original activity is not lost to the organism (*49*), whereas the latter experiments suggested that gene duplication is not necessarily the first step in the optimization of a promiscuous activity (*50*). A few mutations could enable an enzyme to carry out both its physiological reaction as well as the newly acquired one (*50*).

Our results show that the increased CaaD activity of L8R-4-OT does not substantially diminish the original 4-OT activity. The 50-fold increase in CaaD activity is accompanied only by a ~5-fold decrease in 4-OT activity. As such, the results are consistent with those of Tawfik et al. (*50*). However, it remains unknown whether this level of activity, albeit a 10^9-fold rate enhancement over the uncatalyzed reaction, is sufficient to allow for the growth of a "CaaD-deficient" organism. If it does not, then it seems likely that further optimization of the CaaD activity will have a more detrimental effect on the 4-OT activity because of the fundamental differences between the two reactions. Directed evolution studies of 4-OT to improve the CaaD activity are currently being pursued, and these experiments will shed light on how further improvements in the CaaD activity of 4-OT affect the original activity.

ACKNOWLEDGMENT

Electrospray ionization mass spectrometry (ESI−MS) and matrix-assisted laser desorption−ionization (MALDI) mass spectrometry was performed by the Analytical Instrumentation Facility Core (College of Pharmacy, The University of Texas at Austin) supported by Center Grant ES07784. We also thank Steve D. Sorey (Department of Chemistry and Biochemistry, The University of Texas) for his assistance in acquiring the NMR spectra.

SUPPORTING INFORMATION AVAILABLE

Experimental procedures for the construction of the 4-OT mutants and their overexpression and purification. This material is available free of charge via the Internet at http://pubs.acs.org.

REFERENCES

1. Palmer, D. R. J., Garrett, J. B., Sharma, V., Meganathan, R., Babbitt, P. C., and Gerlt, J. A. (1999) Unexpected divergence of enzyme function and sequence: "*N*-Acylamino acid racemase" is *o*-succinylbenzoate synthase, *Biochemistry 38*, 4252−4258.

2. James, L. C., and Tawfik, D. S. (2001) Catalytic and binding polyreactivities shared by two unrelated proteins: The potential role of promiscuity in enzyme evolution, *Protein Sci. 10*, 2600−2607.
3. O'Brien, P. J., and Herschlag, D. (2001) Functional interrelationships in the alkaline phosphatase superfamily: Phosphodiesterase activity of *Escherichia coli* alkaline phosphatase, *Biochemistry 40*, 5691−5699.
4. Wang, S. C., Johnson, W. H., Jr., and Whitman, C. P. (2003) The 4-oxalocrotonate tautomerase- and YwhB-catalyzed hydration of 3*E*-haloacrylates: Implications for evolution of new enzymatic activities, *J. Am. Chem. Soc. 125*, 14282−14283.
5. Poelarends, G. J., Serrano, H., Johnson, W. H., Jr., Hoffman, D. W., and Whitman, C. P. (2004) The hydratase activity of malonate semialdehyde decarboxylase: Mechanistic and evolutionary implications, *J. Am. Chem. Soc. 126*, 15658−15659.
6. Yew, W. S., Akana, J., Wise, E. L., Rayment, I., and Gerlt, J. A. (2005) Evolution of enzymatic activities in the orotidine 5′-monophosphate decarboxylase suprafamily: Enhancing the promiscuous D-arabino-hex-3-ulose 6-phosphate synthase reaction catalyzed by 3-keto-L-gulonate 6-phosphate decarboxylase, *Biochemistry 44*, 1807−1815.
7. Roodveldt, C., and Tawfik, D. S. (2005) Shared promiscuous activities and evolutionary features in various members of the amidohydrolase superfamily, *Biochemistry 44*, 12728−12736.
8. Jensen, R. A. (1976) Enzyme recruitment in evolution of new function, *Ann. Rev. Microbiol. 30*, 409−425.
9. Hughes, A. L. (1994) The evolution of functionally novel proteins after gene duplication, *Proc. R. Soc. London, Ser. B 256*, 119−124.
10. O'Brien, P. J., and Herschlag, D. (1999) Catalytic promiscuity and the evolution of new enzymatic activities, *Chem. Biol. 6*, R91−R105.
11. Schmidt, D. M. Z., Mundorff, E. C., Dojka, M., Bermudez, E., Ness, J. E., Govindarajan, S., Babbitt, P. C., Minshull, J., and Gerlt, J. A. (2003) Evolution potential of $(\beta/\alpha)_8$-barrels: Functional promiscuity produced by single substitutions in the enolase superfamily, *Biochemistry 42*, 8387−8393.
12. Aharoni, A., Gaidukov, L., Khersonsky, O., McQ Gould, S., Roodveldt, C., and Tawfik, D. S. (2005) The "evolvability" of promiscuous protein functions, *Nat. Genet. 37*, 73−76.
13. Whitman, C. P. (2002) The 4-oxalocrotonate tautomerase family of enzymes: How nature makes new enzymes using a $\beta-\alpha-\beta$ structural motif, *Arch. Biochem. Biophys. 402*, 1−13.
14. Poelarends, G. J., and Whitman, C. P. (2004) Evolution of enzymatic activity in the tautomerase superfamily: Mechanistic and structural studies of the 1,3-dichloropropene catabolic enzymes, *Bioorg. Chem. 32*, 376−392.
15. Almrud, J. J., Kern, A. D., Wang, S. C., Czerwinski, R. M., Johnson, W. H., Jr., Murzin, A. G., Hackert, M. L., and Whitman, C. P. (2002) The crystal structure of YdcE, a 4-oxalocrotonate tautomerase homologue from *Escherichia coli*, confirms the structural basis for oligomer diversity, *Biochemistry 41*, 12010−12024.
16. Poelarends, G. J., Serrano, H., Person, M. D., Johnson, W. H., Jr., Murzin, A. G., and Whitman, C. P. (2004) Cloning, expression, and characterization of a *cis*-3-chloroacrylic acid dehalogenase: Insights into the mechanistic, structural, and evolutionary relationship between isomer-specific 3-chloroacrylic acid dehalogenases, *Biochemistry 43*, 759−772.
17. Harayama, S., Rekik, M., Ngai, K.-L., and Ornston, L. N. (1989) Physically associated enzymes produce and metabolize 2-hydroxy-2,4-dienoate, a chemically unstable intermediate formed in catechol metabolism via meta cleavage in *Pseudomonas putida*, *J. Bacteriol. 171*, 6251−6258.
18. Chen L. H., Kenyon G. L., Curtin F., Harayama S., Bembenek M. E., Hajipour G., and Whitman C. P. (1992) 4-Oxalocrotonate tautomerase, an enzyme composed of 62 amino acid residues per monomer, *J. Biol. Chem. 267*, 17716−17721.
19. Whitman, C. P., Aird, B. A., Gillespie, W. R., and Stolowich, N. J. (1991) Chemical and enzymatic ketonization of 2-hydroxymuconate, a conjugated enol, *J. Am. Chem. Soc. 113*, 3154−3162.
20. Poelarends, G. J., Wilkens, M., Larkin, M. J., van Elsas, J. D., and Janssen, D. B. (1998) Degradation of 1,3-dichloropropene by *Pseudomonas cichorii* 170, *Appl. Environ. Microbiol. 64*, 2931−2936.
21. Poelarends, G. J., Saunier, R., and Janssen, D. B. (2001) *trans*-3-Chloroacrylic acid dehalogenase from *Pseudomonas pavonaceae* 170 shares structural and mechanistic similarities with 4-oxalocrotonate tautomerase, *J. Bacteriol. 183*, 4269−4277.
22. Wang, S. C., Person, M. D., Johnson, W. H., Jr., and Whitman, C. P. (2003) Reactions of *trans*-3-chloroacrylic acid dehalogenase with acetylene substrates: Consequences of and evidence for a hydration reaction, *Biochemistry 42*, 8762−8773.
23. Subramanya, H. S., Roper, D. I., Dauter, Z., Dodson, E. J., Davies, G. J., Wilson, K. S., and Wigley, D. B. (1996) Enzymatic ketonization of 2-hydroxymuconate: Specificity and mechanism investigated by the crystal structures of two isomerases, *Biochemistry 35*, 792−802.
24. Taylor, A. B., Czerwinski, R. M., Johnson, W. H., Jr., Whitman, C. P., and Hackert M. L. (1998) Crystal structure of 4-oxalocrotonate tautomerase inactivated by 2-oxo-3-pentynoate at 2.4 Å resolution: Analysis and implications for the mechanism of inactivation and catalysis, *Biochemistry* 37, 14692−14700.
25. de Jong, R. M., Brugman, W., Poelarends, G. J., Whitman, C. P., and Dijkstra, B. W. (2004) The X-ray structure of *trans*-3-chloroacrylic acid dehalogenase reveals a novel hydration mechanism in the tautomerase superfamily, *J. Biol. Chem. 279*, 11546−11552.
26. Stivers, J. T., Abeygunawardana, C., Mildvan, A. S., Hajipour, G., Whitman, C. P., and Chen, L. H. (1996) Catalytic role of the amino-terminal proline in 4-oxalocrotonate tautomerase: Affinity labeling and heteronuclear NMR studies, *Biochemistry 35*, 803−813.
27. Stivers, J. T., Abeygunawardana, Mildvan, A. S., Hajipour, G., and Whitman, C. P. (1996) 4-Oxalocrotonate tautomerase: pH dependences of catalysis and pK_a values of active site residues, *Biochemistry 35*, 814−823.
28. Azurmendi, H. F., Wang, S. C., Massiah, M. A., Poelarends, G. J., Whitman, C. P., and Mildvan, A. S. (2004) The roles of active-site residues in the catalytic mechanism of *trans*-3-chloroacrylic acid dehalogenase: A kinetic, NMR, and mutational analysis, *Biochemistry 43*, 4082−4091.
29. Keuning, S., Janssen, D. B., and Whitholt, B. (1985) Purification and characterization of hydrolytic haloalkane dehalogenase from *Xanthobacter autotrophicus* GJ10, *J. Bacteriol. 163*, 635−639.
30. Weber, D. J., Abeygunawardana, C., Bessman, M. J., and Mildvan, A. S. (1993) Secondary structure of the MutT enzyme as determined by NMR, *Biochemistry 32*, 13081−13088.
31. Otwinowski, Z., and Minor, W. (1997) Processing of X-ray diffraction data collected in oscillation mode, *Methods Enzymol. 276*, 307−326.
32. Matthews, B. W. (1968) Solvent content of protein crystals, *J. Mol. Biol. 33*, 491−497.
33. Vagin, A., and Teplyakov, A. (1997) MOLREP: An automated program for molecular replacement, *J. Appl. Crystallogr. 30*, 1022−1025.
34. Collaborative Computational Project, Number 4. (1994) The CCP4 suite: programs for protein crystallography, *Acta Crystallogr., Sect. D: Biol. Crystallogr. 50*, 760−763.
35. Murshudov, G. N., Vagin, A. A., and Dodson, E. J. (1997) Refinement of macromolecular structures by the maximum-likelihood method, *Acta Crystallogr., Sect. D: Biol. Crystallogr. 53*, 240−255.
36. Brunger, A. T., Adams, P. D., Clore, G. M., DeLano, W. L., Gros, P., Grosse-Kunstleve, R. W., Jiang, J. S., Kuszewski, J., Nilges, M., Pannu, N. S., Read, R. J., Rice, L. M., Simonson, T., and Warren, G. L. (1998) Crystallography and NMR system: A new software suite for macromolecular structure determination, *Acta Crystallogr., Sect. D: Biol. Crystallogr. 54*, 905−921.
37. Laskowski, R. A., MacArthur, M. W., Moss, D. S., and Thornton, J. M. (1993) PROCHECK: A program to check the stereochemical quality of protein structures, *J. Appl. Crystallogr. 26*, 283−291.
38. Kraulis, P. J. (1991) MOLSCRIPT: A program to produce both detailed and schematic plots of protein structures, *J. Appl. Crystallogr. 24*, 946−950.
39. Merritt, E. A., and Murphy, M. E. (1994) Raster3D version 2.0. A program for photorealistic molecular graphics, *Acta Crystallogr., Sect. D: Biol. Crystallogr. 50*, 869−873.
40. Czerwinski, R. M., Harris, T. K., Massiah, M. A., Mildvan, A. S., and Whitman, C. P. (2001) The structural basis for the perturbed pK_a of the catalytic base in 4-oxalocrotonate tautomerase: Kinetic and structural effects of mutations of Phe-50, *Biochemistry 40*, 1984−1995.
41. Harris, T. K., Czerwinski, R. M., Johnson, W. H., Jr., Legler, P. M., Abeygunawardana, C., Massiah, M. A., Stivers, J. T.,

Whitman, C. P., and Mildvan, A. S. (1999) Kinetic, stereochemical, and structural effects of mutations of the active site arginine residues in 4-oxalocrotonate tautomerase, *Biochemistry 38*, 12343−12357.
42. Murzin, A. G. (1996) Structural classification of proteins: New superfamilies, *Curr. Opin. Struct. Biol. 6*, 386−394.
43. Poelarends, G. J., Johnson, W. H., Jr., Murzin, A. G., and Whitman, C. P. (2003) Mechanistic characterization of a bacterial malonate semialdehyde decarboxylase: Identification of a new activity in the tautomerase superfamily, *J. Biol. Chem. 278*, 48674−48683.
44. Rosengren, E., Aman, P., Thelin, S., Hansson, C., Ahlfors, S., Bjork, P., Jacobsson, L., and Rorsman, H. (1997) The macrophage migration inhibitory factor MIF is a phenylpyruvate tautomerase, *FEBS Lett. 417*, 85−88.
45. Sparnins, V. L., Chapman, P. J., and Dagley, S. (1974) Bacterial degradation of 4-hydroxyphenylacetic acid and homoprotocatechuic acid, *J. Bacteriol. 120*, 159−167.
46. Almrud, J. J., Poelarends, G. J., Johnson, W. H., Jr., Serrano, H., Hackert, M. L., and Whitman, C. P. (2005) Crystal structures of the wild-type, P1A mutant, and inactivated malonate semialdehyde decarboxylase: A structural basis for the decarboxylase and hydratase activities, *Biochemistry 44*, 14818−14827.
47. Suzuki, M., Sugimoto, H., Nakagawa, A., Tanaka, I., Nishihira, J., and Sakai, M. (1996) Crystal structure of the macrophage migration inhibitory factor from rat liver, *Nat. Struct. Biol. 3*, 259−266.
48. Horvat, C. M., and Wolfenden, R. V. (2005) A persistent pesticide residue and the unusual catalytic proficiency of a dehalogenating enzyme, *Proc. Natl. Acad. Sci. U.S.A.* 102, 16199−16202.
49. Vick, J. E., Schmidt, D. M. Z., and Gerlt, J. A. (2005) Evolutionary potential of $(\beta/\alpha)_8$-barrels: In vitro enhancement of a "new" reaction in the enolase superfamily, *Biochemistry 44*, 11722−11729.
50. Gould, S. M., and Tawfik D. S. (2005) Directed evolution of the promiscuous esterase activity of carbonic anhydrase II, *Biochemistry 44*, 5444−5452.

BI0600603